

# The Influence of Saturated Steam on Moso Bamboo Quasi-static Micromechanical Properties: Nano-Scale Evaluation

**Tiancheng Yuan**

Nanjing Forestry University

**Zhaoshun Wang**

Nanjing Forestry University

**Xin Han**

Nanjing Forestry University

**ZhuRun Yuan**

Nanjing Forestry University

**XinZhou Wang**

Nanjing Forestry University

**yanjun Li** (✉ [lyj\\_njfu@163.com](mailto:lyj_njfu@163.com))

Nanjing Forestry University

---

## Research Article

**Keywords:** Moso bamboo, saturated steam, modulus of elastic, hardness

**Posted Date:** June 28th, 2021

**DOI:** <https://doi.org/10.21203/rs.3.rs-590616/v1>

**License:** © ⓘ This work is licensed under a Creative Commons Attribution 4.0 International License.

[Read Full License](#)

---

1 *Article*

# 2 **The influence of Saturated Steam on Moso** 3 **Bamboo Quasi-static Micromechanical Properties:** 4 **Nano-Scale Evaluation**

5 **Tiancheng Yuan<sup>1</sup>, Zhaoshun Wang<sup>1</sup>, Xin Han<sup>1</sup>, ZhuRun Yuan<sup>1</sup>, XinZhou**  
6 **Wang<sup>1,2,\*</sup> and Yanjun Li<sup>1,2,\*</sup>**

7 <sup>1</sup> College of Materials Science and Engineering, Nanjing Forestry University, Nanjing 210037,  
8 China; tc\_yuan@njfu.edu.cn (T.Y.); zhaoshun\_wang@njfu.edu.cn (Z.W.);  
9 xinhan2019@njfu.edu.cn (X.H.); yuanzr0311@njfu.edu.cn (R.Y.);

10 <sup>2</sup> Jiangsu Co-Innovation Center of Efficient Processing and Utilization of Forest Resources,  
11 Nanjing 210037, China

12 \* Correspondence: xzwang@njfu.edu.cn (Z.W.); lalyj@njfu.edu.cn (Y.L.)

13 Received: date; Accepted: date; Published: date

## 14 **Abstract:**

15 In this paper, in order to analyze the quasi-static properties of Moso bamboo, a  
16 new, environmentally friendly and eco-friendly method was used for bamboo thermal  
17 modification under the effect of saturated steam. Under saturated steam heat treatment,  
18 the chemical composition in bamboo decreased, and the bamboo cell wall shrunk  
19 slightly. The increased crystallinity index of cellulose and decreased intensity of peaks  
20 belong to hemicellulose were confirmed by XRD and Fourier transform infrared (FTIR)  
21 spectroscopy. In addition, the highest modulus of elastic and hardness of treated  
22 bamboo were 22.5GPa and 1.1GPa at 180°C/10 min. These conclusions confirmed the  
23 micro-mechanical properties of the bamboo cell wall were enhanced by saturated steam  
24 heat treatment. The  $E_r'$  of differently treated bamboo increased with increasing  
25 temperature and time, while the  $E_r''$  and  $\tan \delta$  negatively as a function of increasing  
26 frequency. Furthermore, this thermal modification can be regarded as a useful,  
27 environmental-friendly and eco-friendly treatment to outdoor use of bamboo-based  
28 materials.

29 **Keywords:** Moso bamboo; saturated steam; modulus of elastic; hardness.

## 30 **1. Introduction**

31 Bamboo belongs to the Gramineae family and has been widely used in many fields  
32 in our daily life, such as furniture, construction, and so forth (**Wang et al. 2019b; Yuan**  
33 **et al. 2020; Wang et al.**). Scientific and reasonable application of bamboo can  
34 effectively reduce the demand for the woody resource(**Zhang et al. 2013**). On this  
35 respect, more attention has been paid to bamboo due to its excellent mechanical  
36 properties, fast growth, and stable performance(**Li et al. 2015; Tang et al. 2019**).  
37 However, bamboo is easily affected by fungi, moisture, and injurious insect due to its  
38 abundance in polysaccharides and starch, which limits the outdoor utilization of  
39 bamboo-based products. Meanwhile, when bamboo-based engineered bamboo  
40 materials are applied for long-term usage, it is easy to produce problems like short  
41 product life, low dimensional stability, and low resistance to biodegradation. So, it is  
42 of great importance to improving the physical and mechanical properties of bamboo to  
43 solve the above problems.

44 Thermal modification has been widely applied in making bamboo-based products,  
45 which can effectively improve the physical and mechanical properties of bamboo  
46 products. The aim of thermal modification is to change the polysaccharide and starch  
47 content and microstructure of bamboo tissue, to improve the macro-mechanical  
48 properties such as color (aesthetic purposes), modulus of elasticity, equilibrium  
49 moisture content, and so on. The inert gas, water, and oil were the three main traditional  
50 heat treatment mediums that the treatment temperature and treatment time in the range  
51 of 150°C – 250°C, and 2 – 6 h, respectively. However, traditional thermal modification  
52 leads to the evaporation completely of moisture content in bamboo, which leads to a  
53 negative effect on the macro-mechanical properties of bamboo with increasing severity  
54 of treatment. Therefore, scientists are urgent to find a rapid and gentle heat treatment  
55 medium for the modification of bamboo. Saturated steam is steam that is controlled by  
56 pressure and at a temperature lower than the boiling point. Thus, saturated steam heat  
57 treatment can provide a high temperature and high humidity environment for  
58 modification simultaneously. It is of great interest to study the mechanical properties  
59 of bamboo in nanoscale and microscale ranges.

60 Previous literatures focus on the macroscale properties and surface changes of  
61 moso bamboo after thermal modification. For example, **Wang et al** studied the  
62 influence of saturated steam pretreatment on the drying quality of bamboo culms,

63 results showed that saturated steam can effectively improve the drying quality of  
64 bamboo culms and reduce cracks. However, he did not reveal the reason from nano-  
65 scale perspective. Micro-level study are rare in this field. **Wang Q et al** studied the  
66 effects of different treatment temperature and time on the mechanical and chemical  
67 composition of moso bamboo with different initial moisture contents. **Yuan T et al**  
68 reveled the infulence of different treatment parameters on equilibrium moisture content,  
69 oven-dried density, and color on moso bamboo. So, the study of effect of saturated  
70 steam on moso bamboo in nano-scale are rare. In addition, Quasi-static indentation was  
71 used to characterizes the micro-mechanical properties of biomass materials such as  
72 wood, bamboo, and straw by means of nanoindentation(**He et al. 2019a, b; Guan et**  
73 **al. 2020**). It is also a successful approach for determining the modulus of elasticity and  
74 hardness of a single cell wall. In addition, for the application of bamboo in oscillation  
75 stress and long-term bearing, viscoelastic is an interesting topic. For this purpose,  
76 Nanoindentation technology is applied for analyzing these problems and is suited to  
77 this purpose. Moreover, combining quasi-static indentation and other modern test  
78 instruments can deeply understand the nanomechanical properties of bamboo cell wall.

79 In this paper, the bamboo is heat-treated by saturated steam at different  
80 temperatures and times and then analyzed by means of Fourier transform infrared  
81 (FTIR) spectroscopy, environmental scanning electron microscope (SEM), X-ray  
82 diffraction (XRD), wet chemistry method, and quasi-static Nanoindentation.

## 83 **2. Materials and methods**

### 84 **2.1. Materials preparation**

85 Natural three-year-old Moso Bamboo (*Phyllostachys pubescens*) with average  
86 dimensions of 50\*20\*t mm (length \* width \* wall thickness) were collected from  
87 JiangXi Province, China. The initial moisture content of samples was 90%. bamboo  
88 culms were subjected to heat treatment at different temperatures (160, 180°C) for  
89 different periods (15, 30min).The bamboo culms were placed in pressurized steam  
90 equipment. After treatment, all samples were placed in a constant temperature and  
91 humidity equipment (HWS-250, Jinhong Co., Ltd., China) for 2 weeks under 20°C and  
92 65% (relative humidity).

### 93 **2.2. X-ray diffraction (XRD) analysis**

94 The different treated bamboo specimens were ground into powder and sieved  
95 through an 80 mesh screen. The samples were then placed in an oven for 12 hours until  
96 the moisture content was 0%. Then, the XRD method (Ultima-IV combination X-ray  
97 diffractometer, Japan) was utilized to analyze the crystallinity of bamboo cellulose at  
98 different treatment temperatures and times. Data were collected in the 2-theta scanning  
99 range from 10° to 80°. Based on Segal's formula, the XRD analysis results constituted  
100 the average of three replicate experiments, and relative crystallinity can be calculated  
101 as below:

$$C_r I = (I_{002} - I_{am}) / I_{002} \times 100\%, \quad (1)$$

102 where CrI represents the relative content of crystallinity, and  $I_{002}$  and  $I_{am}$  denote the  
103 the maximum in the intensity of the (200) peak and the minimum in the intensity  
104 between the overlapped  $(1\bar{1}0)/(110)$  and the (200) peak.

### 105 **2.3. Fourier transform infrared spectroscopy (FTIR)**

106 The powders used in XRD analysis were also used to FTIR analysis on a FTIR  
107 spectrometer (500-4000  $\text{cm}^{-1}$  range, 32 accumulations, 2  $\text{cm}^{-1}$  resolution; Bruker  
108 Corporation, Karlsruhe, Germany). KBr Pellet Method were used to further analyze the  
109 chemical functional groups. The FTIR analysis for each sample was based on averages  
110 of three replicate experiments.

### 111 **2.4. Oven-dried density and mass loss**

112 The treated and untreated bamboo were possessed into the average size of 10\*10\*T  
113 mm (length\*width\*thickness) and the density was tested by oven-drying method. Ten  
114 samples were repeatedly collected from each group for analysis The percentage of mass  
115 loss following saturated steam heat treatment was calculated by formula as below:

$$\%ML = 100 (M_0 - M_1) / M_0 \quad (2)$$

116 Where  $m_0$  represents the initial oven-dried specimen mass,  $m_1$  represents the  
117 oven-dried specimen mass after saturated steam heat treatment

### 118 **2.5. Chemical compositions analysis**

119 In this step, the treated bamboo samples were ground and screened into powder  
120 using 40 and 80 screens. The main chemical composition (cellulose, hemicellulose, and  
121 lignin content) of samples was determined and calculated according to NREL'S LAPs.  
122 All data were represented as averages of three replicate experiments, closest to 0.1%.

## 123 **2.6. Nanoindentation (NI)**

124 Samples treated by saturated steam, together with untreated samples, were  
125 processed into small blocks of  $0.5 * 0.5 * 1\text{mm}^3$ , the cross-section of bamboo samples  
126 were polished by a diamond knife, as shown in Figure 1, five samples were placed  
127 under constant temperature ( $21\pm 1^\circ\text{C}$ ) and humidity ( $65\pm 4\%$ ) for 24 hours before the  
128 tests. NI was performed on a load-controlled mode to obtain at least 30 valid  
129 indentations (see Figure 1). Loading was performed within 5s, the holding time was 5s,  
130 and unloading terminated within 5s. A peak load ( $400\mu\text{N}$ ) were applied to all indents.  
131 All data were averages of 30 valid data.

## 132 **2.7. Elastic modulus and hardness**

133 Based on the formula according to Oliver (1992), the reduced elastic modulus and  
134 hardness can be calculated as formula follows:

$$H = \frac{P_{max}}{A} \quad (3)$$

135 where  $P_{max}$  is the peak load, and A denotes the projected contact area of the indents at  
136 peak load.

$$Er = \frac{\sqrt{\pi} S}{2\beta \sqrt{A}} \quad (4)$$

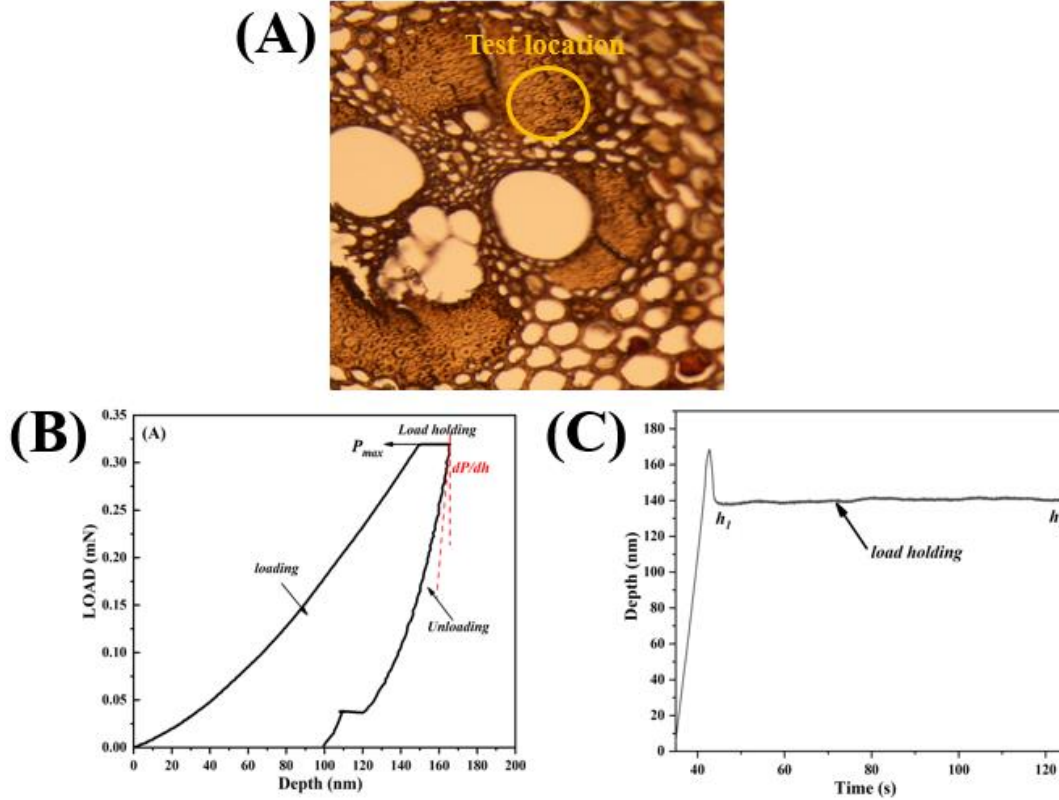
137 where  $Er$ ,  $S(dP/dh)$ , and  $\beta$  represent the combined elastic modulus of both the  
138 specimen and indenter, the initial unloading stiffness, and the correction factor to indent  
139 geometry ( $\beta = 1.034$ ), respectively.

## 140 **2.8. Creep behavior**

141 In order to investigate the creep behavior of bamboo, specimens were held for 200s  
142 after uploading by a maximum load of  $400\mu\text{N}$ . Creep behavior can be calculated from  
143 the load-indentation depth graph based on Konnerth and Gindl's method.

$$C_{IT}(\%) = \frac{h_2 - h_1}{h_1} \times 100 \quad (8)$$

144 where  $h_2$  and  $h_1$  represent the final and first penetration depth of the segment,  
 145 respectively.



146

147 **Figure 1.** (A) Test area; Typical NI representative load-depth(B) and depth-time(C)  
 148 curves of the bamboo fiber cell.

## 149 2.9. Dynamic mechanical properties analysis

150 After the test of nanoindentation, the nanoDMA tests were tested by the same  
 151 indenter and operated in a ramping dynamic frequency mode. The quasi-static load and  
 152 the dynamic load was equal to 100  $\mu$ N and 10  $\mu$ N, respectively. The frequencies were  
 153 ranged from 10 to 200 Hz and each frequency has 100 cycles. Data were collected from  
 154 30 valid indentations which were tested in five or six cells. The  $E'_r$  and  $E''_r$  were  
 155 calculated based on Chakravartula and Komvopoulos's method

$$E'_r = \frac{K_S \sqrt{\pi}}{2\sqrt{A}} \quad (9)$$

$$E''_r = \frac{wC_S \sqrt{\pi}}{2\sqrt{A}} \quad (10)$$

156

$$\tan \delta = \frac{C_s W}{k_s} \quad (11)$$

157 Where A,  $k_s$ , and  $C_s$  represents the projected area of the contact, contact stiffness and  
158 the damping coefficient of the sample, respectively.

159 The  $K_s$  can be calculated as below:

$$K_s = K - K_1 \quad (12)$$

160 Where  $K$ , and  $K_1$  is the combined stiffness and the spring constant of the leaf  
161 springs holding the indenter shaft, respectively.

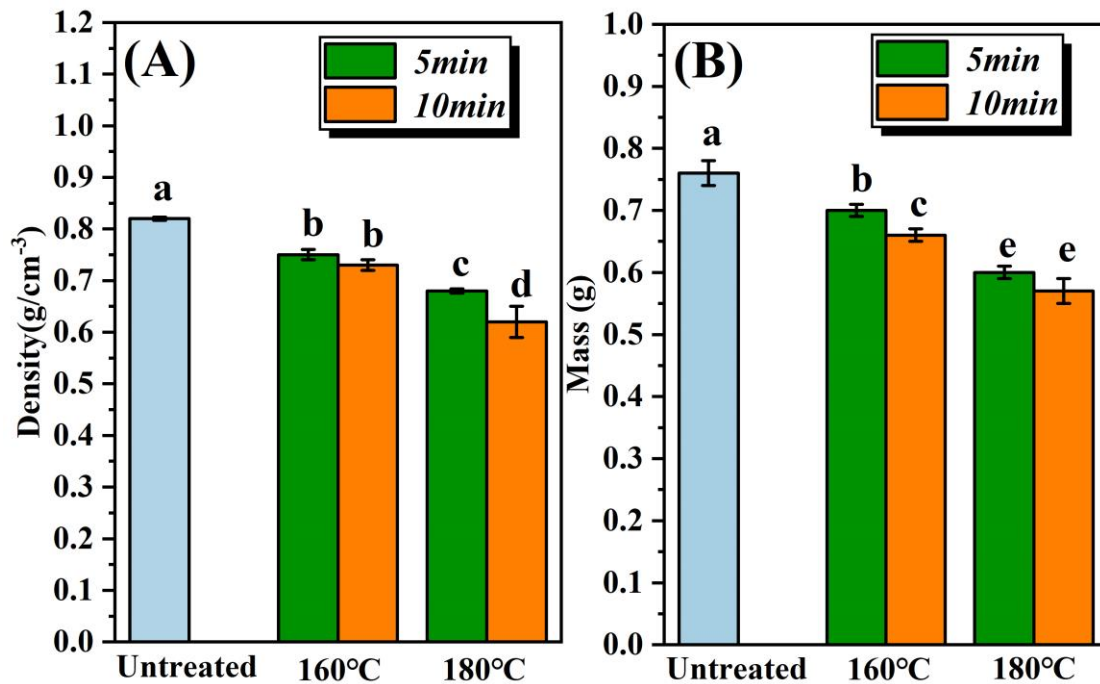
## 162 **2.10 Data analysis**

163 All data were statistically analyzed using SPSS software. Duncan multiple range test  
164 were performed to analysis significant influence between groups. In this paper, different  
165 lowercase letters represents significant differences between groups.

## 166 **3. Results and discussion**

### 167 **3.1 Oven-dried density and mass analysis**

168 Results for oven-dried density, mass after saturated steam heat treatment of  
169 differently treated bamboo samples are shown in Figure2. Density and mass for  
170 untreated bamboo was found to be  $0.82\text{g/cm}^3$  and  $0.76\text{g}$ , respectively. Expectedly, the  
171 density and mass decreased with an increase in treatment temperature and time.  
172 According to previous literature, which is attributed to the degradation of  
173 polysaccharides in the cell wall(Huang et al. 2018). In addition. The loss of volatile  
174 composition from extractives may also contribute to these observations when the  
175 treatment temperature above  $160^\circ\text{C}$ (Zhu et al. 2020).



176

177

**Figure 2.** density and mass analysis of untreated and saturated-steam heat treatment sample The different letters represent significant differences between treatments ( $p < 0.05$ ).

178

179

### 3.2 Microstructure

180

As shown in Figure 3 (A-C), SEM was applied for analyzing different treated bamboo samples. The microstructure of bamboo is totally different from wood. Bamboo is a natural material composed by two main components (vascular bundles and parenchyma cells). Parenchyma cell is the principal matrix of bamboo. Figure 3A shows the thin-wall cells exhibited spongiform and porous characteristics and vascular bundles is solid areas with hollow tubes. Figure 3B (1-3) illustrates that the volume of parenchyma cell became smaller after saturated steam heat treatment (160°C/15min). In addition, slightly shrank appeared in the thin-walled cells. Increased treatment temperature contributed to this phenomenon. Figure 3 (C) shows a visual comparison of the cross-section section of pre-and post-treatment bamboo samples. It can be observed from figure 3C that the parenchyma cells and vascular bundles have been collapsed by the saturated steam heat-treatment process. The separation between vascular bundles and parenchyma cells are obvious from the SEM images. This increase change in the bamboo cell wall is associated with increasing treatment temperature.

181

182

183

184

185

186

187

188

189

190

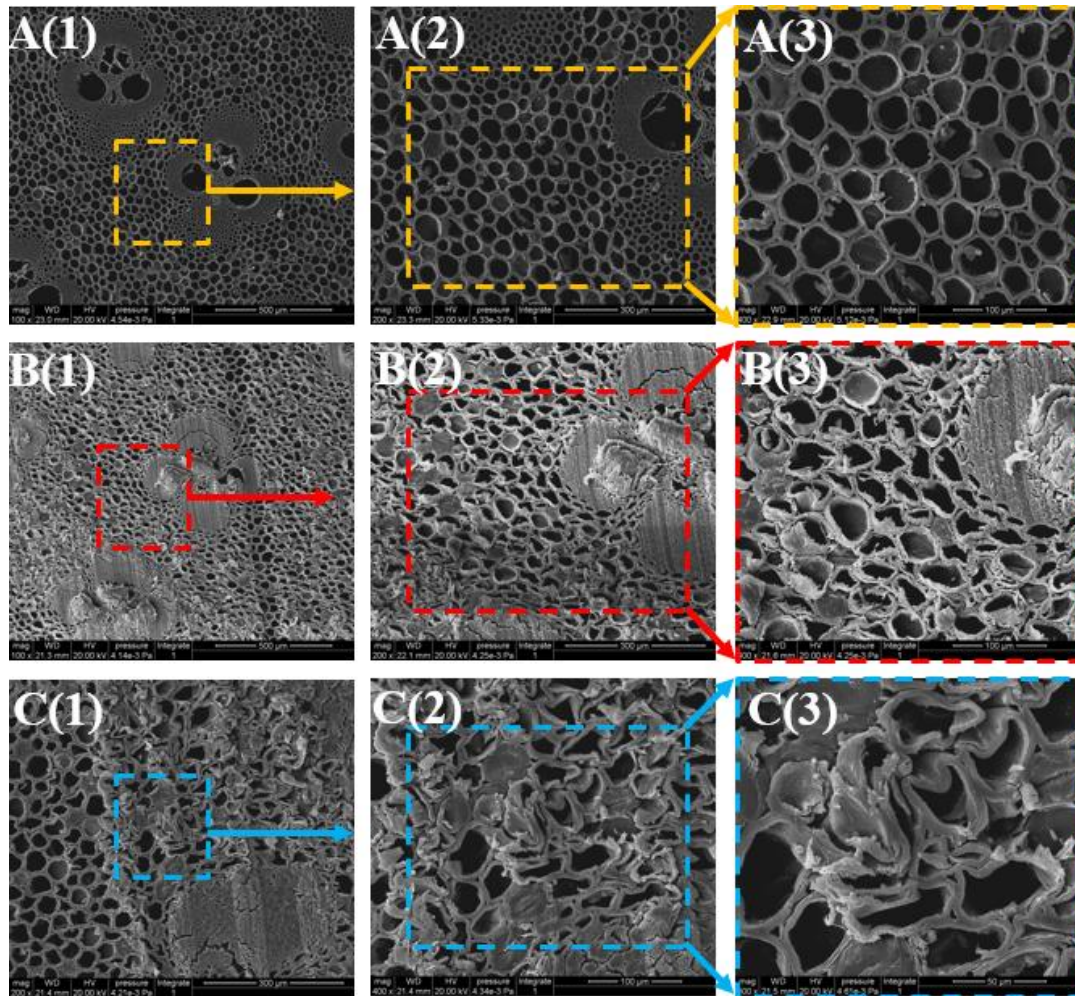
191

192

193

194

195 Additionally, the decomposition of polysaccharides in bamboo cell wall is another  
196 reason for this conclusion.



197  
198 Figure 3: SEM images of cross-section different treated bamboo: (A) untreated; (B)  
199 160°C/10min; (C) 180°C/10min

### 200 3.3 Main chemical composition

201 As shown in table 1, Due to thermal modification (TM) the hemicellulose content  
202 was negatively correlated with treatment severity. In addition, the content of cellulose  
203 was also negatively affected by heat treatment. Following treatment under 180°C for  
204 10 min, the relative hemicellulose content (19.7%) was reduced by around 7.8%  
205 compared with that of the untreated sample. This observation is in agreement with the  
206 previous literature. Xylan, the main component of hemicellulose, is sensitive to high-  
207 temperature conditions and is subjected to dehydration reactions(Ohmae et al. 2009).  
208 Moreover, the lignin content showed an increasing trend with the decrease of  
209 hemicellulose and cellulose levels. The lignin content observed upon 180°C for 10min  
210 was significant at 32.5%, which was a 4.1% increment of that of control. This finding

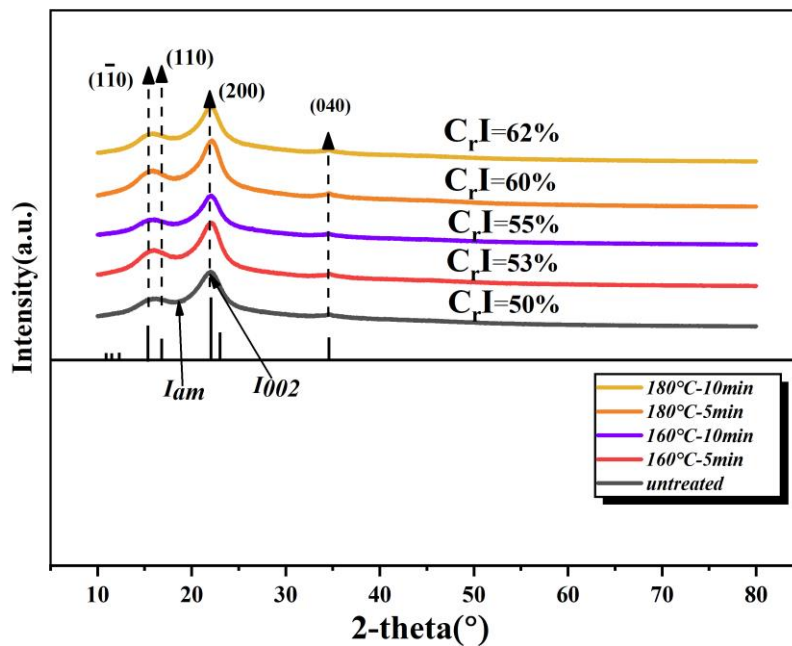
211 supports previous conclusions in the literature. This is due to the condensation of  
 212 hemicellulose by-products with lignin conducive to this phenomenon. In addition,  
 213 considering the low thermal stability of polysaccharides in hemicellulose resulting from  
 214 the branched and amorphous structure, it can be attributed to the hemicellulose in  
 215 bamboo is easier to decompose than cellulose or lignin(Zhang et al. 2013). Furthermore,  
 216 the conclusion of the reduction in hemicellulose' content in fiber cells was also  
 217 confirmed by SEM.

218 **Table 1.** Relative contents of hemicellulose, cellulose, and lignin in the samples obtained  
 219 after saturated-steam heat treatment.

Time	Cellulose		Hemicellulose		Lignin	
	160°C	180°C	160°C	180°C	160°C	180°C
Untreated	36.9		25.6		27.3	
5min	33.5	32.4	23.3	22.5	29.9	30.4
10min	30.3	28.3	21.5	19.7	30.3	32.5

### 220 **3.4 XRD analysis**

221 Cellulose, the main composition of bamboo, is the main reason for the strength of  
 222 lignocellulose materials. As it is known to all, the amorphous and crystalline region  
 223 are two main components of cellulose and their relationship further influence the  
 224 micromechanical properties of the bamboo cell wall. Figure 4 shows the XRD patterns  
 225 and degree of crystallinity of different treated bamboo specimens. The crystallinity  
 226 indexes were obtained by Eq.1. Expectedly, the degree of crystallinity increased after  
 227 saturated steam heat treatment. Both treatment temperature and duration clearly made  
 228 a positive impact on the relative crystallinity of cellulose, while the mean CrI value of  
 229 the untreated sample was 50%. As shown in Figure 4, the relative degree of  
 230 crystallinity was positively correlated with thermal modification severity. In other  
 231 words, both temperature and duration positively contributed to crystallinity. The  
 232 obvious increment in the CrI was specimens treated at 180°C for 10 min. Saturated  
 233 steam treatment at 180°C for 10 min results in higher CrI compared with that of the  
 234 control. the change from 50.0% to 62%, which is a 24% increment, It was attributed  
 235 to the decomposition of hemicellulose. Additionally, the proportion of paracrystalline  
 236 cellulose also decreases due to the acidic environment. Thus, the relative crystallinity  
 237 of bamboo is further increased.



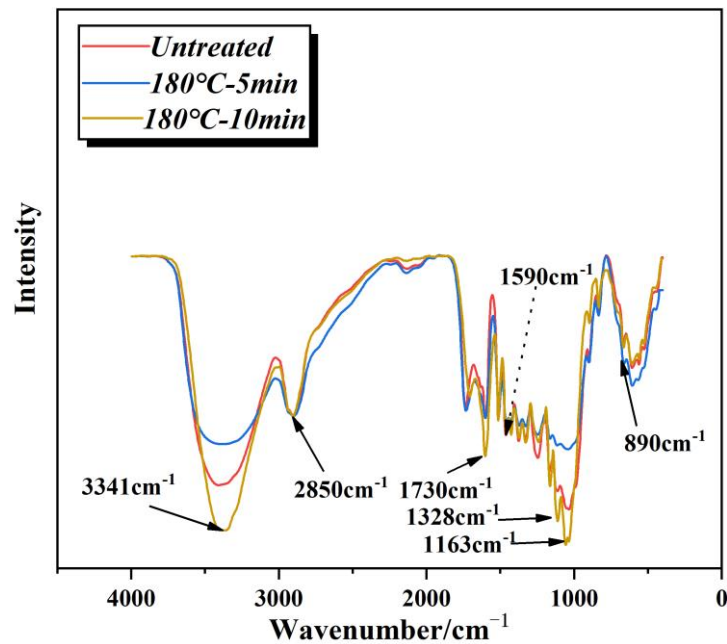
239

240 **Figure 4.** XRD curves and crystallinity index of untreated and different treated sample  
 241 (relatively degree of crystallinity are shown in picture).

### 242 3.5 FTIR analysis

243 FTIR spectroscopy of the untreated bamboo and differently treated bamboo is a  
 244 method to analyze the bamboo chemical components. The relevant data of this study  
 245 are shown in Figure 5. The peak at  $890\text{cm}^{-1}$  can be assigned to C-H, which represents  
 246 C H deformation in cellulose. The  $890\text{ cm}^{-1}$  of samples treated at different temperatures  
 247 did change too much show the main structure of cellulose is still intact. The peak at  
 248  $3341\text{cm}^{-1}$  and  $2850\text{ cm}^{-1}$  represented stretching vibration of -OH and stretching  
 249 vibration of C-H vibration. These two peaks decreased in comparison to that of the  
 250 control. These results illustrated that saturated steam heat treatment decreased the  
 251 hydroxyl groups in bamboo. The  $1730\text{ cm}^{-1}$  peak, which represented C=O stretching  
 252 vibration in hemicellulose, and the intensity of  $1730\text{cm}^{-1}$  decreased, which is maybe the  
 253 decomposition of hemicellulose. The peaks at  $1163\text{ cm}^{-1}$  and  $1328\text{ cm}^{-1}$  correspond to  
 254 C-O-C stretching vibration and O-H stretching vibration, respectively. The visible  
 255 weakening of the above peak ( $1163\text{ cm}^{-1}$  and  $1328\text{ cm}^{-1}$ ) is due to the hydrolysis of  
 256 hemicellulose. Additionally, the characteristic peaks of lignin ( $1590\text{cm}^{-1}$ ) increased,

257 which further confirmed the increase in lignin content. Lignin condensation with by-  
258 products (arise from hydrolysis of hemicellulose) conductive to this phenomenon.



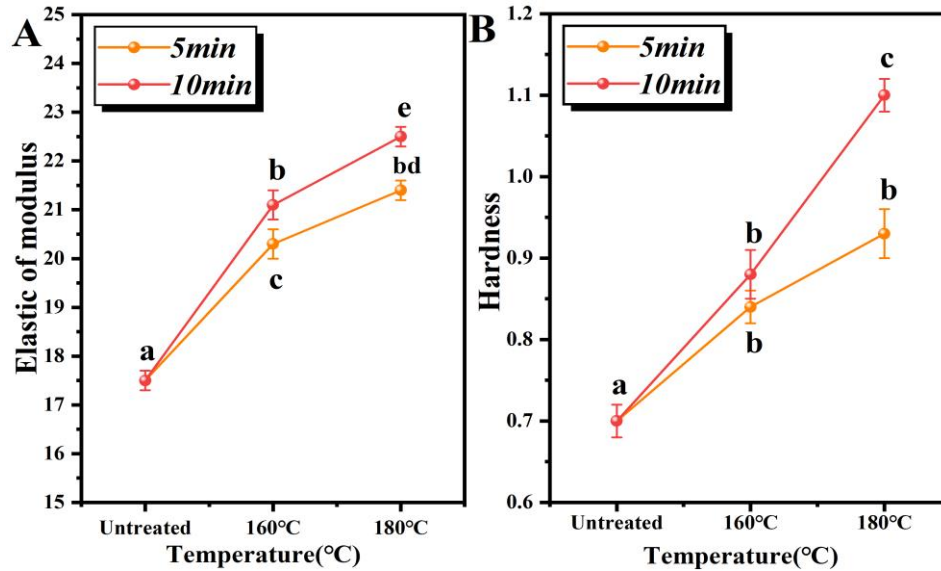
259

260 **Figure 5.** Normalized FTIR curves of bamboo samples at different time and same  
261 temperature.

### 262 3.6 Cell-wall mechanics

263 The elastic modulus and hardness values of different treated samples are shown in  
264 Figure 6. Results present that thermal treatment contribute positively to the stiffness of  
265 bamboo cell wall. For instance, the elastic modulus and hardness values of untreated  
266 bamboo fiber wall was around 17.8 GPa and 0.71 GPa. When treated at 160°C/10min,  
267 elastic modulus and hardness increased by 4.3% and 13.3%, respectively. When the  
268 temperature was set at 180°C for 10min, their values improved by ca.15% and 36%,  
269 respectively. During the process of lignification of bamboo fiber, lignin forms a  
270 amorphous network which can enclose the holocellulose, which can improve the  
271 stiffness of micromechanical properties. Thus, increased lignin content positively  
272 influence the mechanical properties of bamboo cell wall. Increased crystallinity index  
273 and decomposition of hemicellulose may also enhance the mechanical properties as  
274 reported by wang et al. Therefore, this finding is in agreement with the previous  
275 literature(Wang et al. 2017, 2019a, 2020b). Under the conditions of high-temperature  
276 and pressure, such as high-temperature and high pressure saturated steam. The  
277 increased average micromechanical properties of the bamboo cell-wall was partly due

278 to the lignin condensation and partly due to the cross-linking reactions of by-products  
279 which arised from decomposition of hemicelluloses. In this study, elastic modulus and  
280 hardness showed a upward tendency with an increase in treatment temperature and  
281 time.

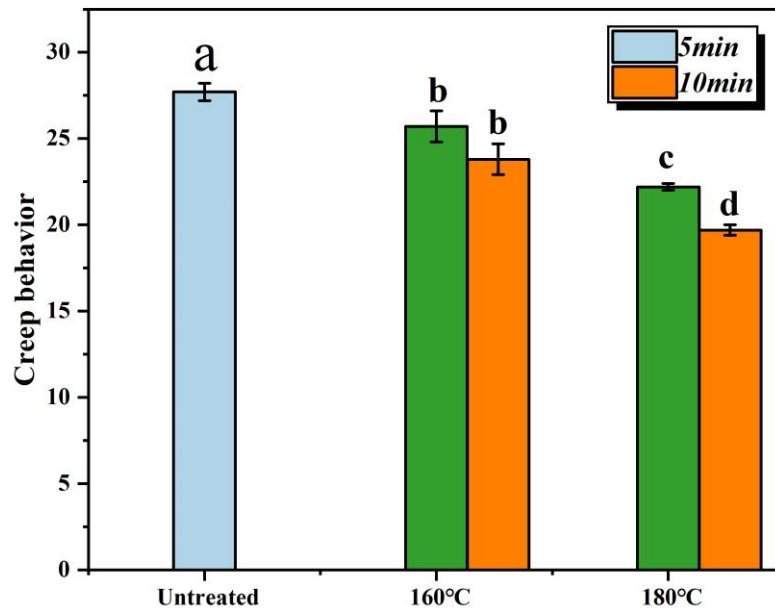


282

283 **Figure 7.** Elastic modulus and hardness of untreated control and bamboo under different temperatures and times  
284 periods. The different letters represent significant differences between treatments ( $p < 0.05$ ).

### 285 3.7 Creep behaviour analysis

286 As a biomass material, bamboo exhibits visco-elasticity. In addition, creep  
287 behavior is an important performance of woody material. The effects of saturated steam  
288 heat treatment on the creep ratio of bamboo cell wall were investigated by  
289 Nanoidentation. As is illustrated in Figure 8. the average creep ratio of the untreated  
290 sample was 27.2%, which was higher than that of the treated bamboo cell wall. In the  
291 same time, the treatment parameters of 180°C/10min obviously decreased the creep  
292 ratio. For example, The lowest creap ratio of bamboo sample was observed at  
293 180°C/10min, which means the resistance of creep improved. Hemicelluloses are  
294 important components that may account for this creep behavior. As discussed above,  
295 when the treatment was performed at 180°C or higher, the treatment severity  
296 contributed to a reduction in the content of hemicelluloses. Hemicellulose plays a  
297 matrix role in the cell wall, which is weakened by the decomposition of hemicellulose  
298 due to the high temperature and pressure condition. The condensation of lignin and the  
299 increased crystallinity may also contribute to this phenomenon (Qu et al. 2020).



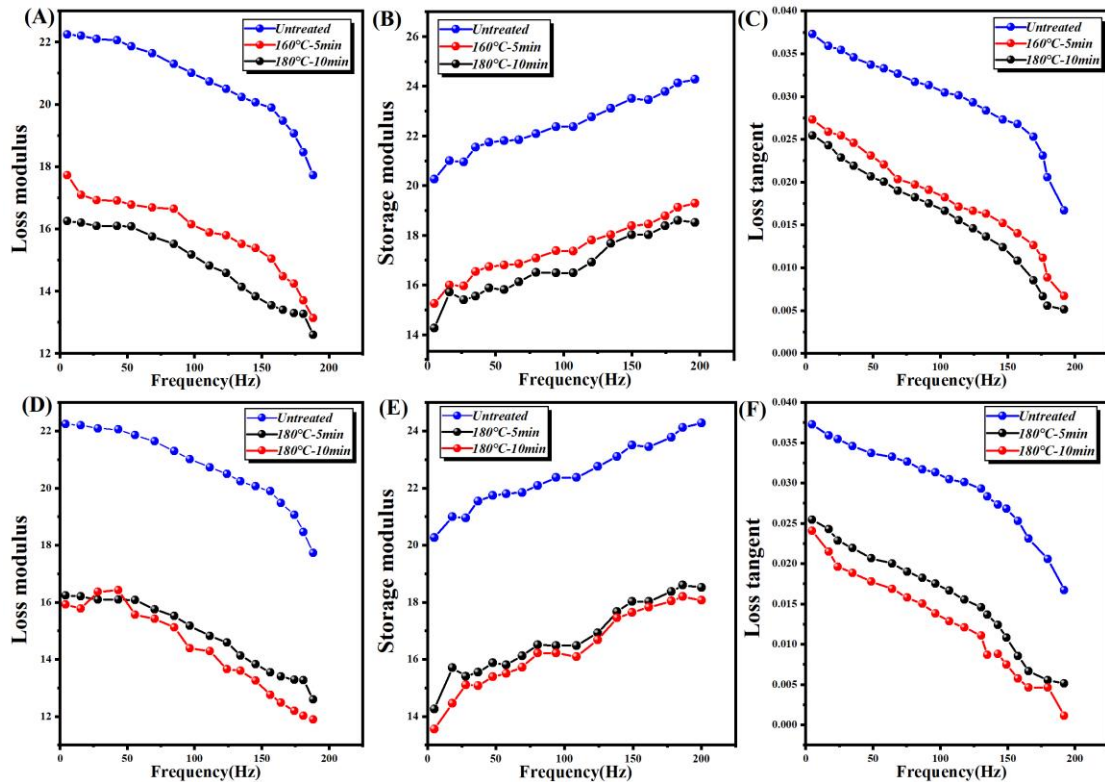
300

301 **Figure 7.** The creep ratios of bamboo fiber wall after saturated steam heat treatment. The different letters represent  
 302 significant differences between treatments ( $p < 0.05$ ).

### 303 **3.8 Dynamic mechanical properties of bamboo fiber wall**

304 Figure.8 represents the relationship between the dynamic indentation of bamboo  
 305 fiber wall and frequency. Accordingly, the loss modulus, storage modulus, and loss  
 306 tangent of differently treated bamboo samples were lower than that of the untreated  
 307 sample, the storage modulus and loss tangent decreased with an increase of temperature,  
 308 which was mainly owing to the fact that the decomposition of hemicellulose and  
 309 melting. In addition, the storage modulus increased slightly with an increase of  
 310 temperature while loss tangent decreased significantly. This is maybe the relationship  
 311 between molecular chains and different frequencies. In detail, lower frequency leads to  
 312 a slight influence on flexible molecular chains; The main chain negatively corresponds  
 313 to frequency, in other the main chain movements decreased with increasing frequency.  
 314 In conclusion, the loss modulus decreased significantly. Enhanced frequency  
 315 contributed negatively to the loss tangent, this is due to the shorter molecular chain  
 316 rearrangement time resulting in the stiffening of material(Yang et al. 2020; Hao et al.  
 317 2021). Figure 8. (D) (E) (F) presents the influence of different frequencies on the  
 318 storage modulus, loss modulus, and loss tangent of different duration treated bamboo

319 samples. Treatment time has slight effect on the dynamic mechanical properties of  
 320 moso bamboo.



321  
 322 Figure.8 The dynamic mechanical properties of bamboo cell-wall at different  
 323 temperature and time. A and D:  $E''$  (loss modulus); B and E:  $E'$  (storage modulus); C  
 324 and F:  $\tan \delta$  (loss tangent).

325 **4. Conclusions**

326 The average density and mass of the saturated steam heat treatment treated  
 327 bamboo decreased with an increase in temperature and time. Saturated steam can  
 328 effectively reduce the content of hemicellulose and increased the crystallinity index.  
 329 The bamboo cell wall shrunk due to the high temperature and high pressure. However,  
 330 the modulus of elastic and hardness of bamboo cell wall increased from 19.8GPa to  
 331 25.5GPa and from 0.68GPa to 1.1GPa due to the increased lignin content and increased  
 332 crystallinity degree. The observation was confirmed by wet chemical method, FTIR,  
 333 XRD, and Nanoindentation. Furthermore, dynamic indentation revealed a decreased  
 334 loss modulus and loss tangent and enhanced storage modulus during thermal  
 335 modification. the  $E'$  of differently treated bamboo increased with increasing  
 336 temperature and time, while the  $E''$  and  $\tan \delta$  negatively as a function of increasing  
 337 frequency.

338 **Author Contributions:** Conceptualization, Y.L; investigation, Z.W, and R.Y.; project  
339 administration Y.L, data curation X.H.and W.S.writing-original draft preparation, T.Y.,  
340 and Z.W. All authors have read and agreed to the published version of the manuscript.

341 **Funding:** This research was funded by the National Natural Science Foundation of  
342 China(NO.31971740 and 31901374), Project of “13th Five-Year” National Key R&D  
343 Plan (2017YFD0600801), Key University Science Research Project of Jiangsu  
344 Province (Grant No.17KJA220004), Zhejiang provincial collaborative innovation  
345 center for bamboo resources and high-efficiency utilization (Grant No.2017ZZY2-06),  
346 forestry science and technology development project of the National Forestry and  
347 Grassland Administration (Grant No. KJZXZZ201900X), key research and  
348 development project of Fujian province (Grant No.2019N3014). A Project Funded by  
349 the Priority Academic Program Development of Jiangsu Higher Education Insitutions  
350 (PAPD), A Project Funded by the National First-class Disciplines (PNFD), Supported  
351 by the Doctorate Fellowship Foundation of Nanjing Forestry University.

352 **Conflicts of Interest:** The authors declare no conflict of interest.

353 Ethical Compliance

354 Research experiments conducted in this article with animals or humans were approved  
355 by the Ethical Committee and responsible authorites of our research organization (s)  
356 following all guidelines, regulations, legal, and ethical standards as required for humans  
357 or animals.

## 358 **Reference**

- 359 Guan M, Tang X, Du K, et al (2020) Fluorescence characterization of the precuring of  
360 impregnated fluffed veneers and bonding strength of scrimber in relation to drying  
361 conditions. *Drying Technology* 1–8. <https://doi.org/10.1080/07373937.2020.1786109>
- 362 Hao X, Wang Q, Wang Y, et al (2021) The effect of oil heat treatment on biological,  
363 mechanical and physical properties of bamboo. *J Wood Sci* 67:26.  
364 <https://doi.org/10.1186/s10086-021-01959-7>
- 365 He Q, Zhan T, Ju Z, et al (2019a) Influence of high voltage electrostatic field (HVEF)  
366 on bonding characteristics of Masson (*Pinus massoniana* Lamb.) veneer composites.  
367 *Eur J Wood Prod* 77:105–114. <https://doi.org/10.1007/s00107-018-1360-6>

368 He Q, Zhan T, Zhang H, et al (2019b) Robust and durable bonding performance of  
369 bamboo induced by high voltage electrostatic field treatment. *Industrial Crops and*  
370 *Products* 137:149–156. <https://doi.org/10.1016/j.indcrop.2019.05.010>

371 Huang X, Xie J, Qi J, et al (2018) Differences in physical–mechanical properties of  
372 bamboo scrimbers with response to bamboo maturing process. *Eur J Wood Prod*  
373 76:1137–1143. <https://doi.org/10.1007/s00107-018-1293-0>

374 Li T, Cheng D, Wålinder MEP, Zhou D (2015) Wettability of oil heat-treated bamboo  
375 and bonding strength of laminated bamboo board. *Industrial Crops and Products* 69:15–  
376 20. <https://doi.org/10.1016/j.indcrop.2015.02.008>

377 Ohmae Y, Saito Y, Inoue M, Nakano T (2009) Mechanism of water adsorption capacity  
378 change of bamboo by heating. *Eur J Wood Prod* 67:13–18.  
379 <https://doi.org/10.1007/s00107-008-0281-1>

380 Qu L, Wang Z, Qian J, et al (2020) Effects of aluminum sulfate soaking pretreatment  
381 on dimensional stability and thermostability of heat-treated wood. *Eur J Wood Prod*.  
382 <https://doi.org/10.1007/s00107-020-01616-8>

383 Tang T, Chen X, Zhang B, et al (2019) Research on the Physico-Mechanical Properties  
384 of Moso Bamboo with Thermal Treatment in Tung Oil and Its Influencing Factors.  
385 *Materials* 12:599. <https://doi.org/10.3390/ma12040599>

386 Wang, Chen, Xie, et al (2019a) Multi-Scale Evaluation of the Effect of Phenol  
387 Formaldehyde Resin Impregnation on the Dimensional Stability and Mechanical  
388 Properties of *Pinus Massoniana* Lamb. *Forests* 10:646.  
389 <https://doi.org/10.3390/f10080646>

390 Wang Q, Wu X, Yuan C, et al (2020a) Effect of Saturated Steam Heat Treatment on  
391 Physical and Chemical Properties of Bamboo. *Molecules* 25:1999.  
392 <https://doi.org/10.3390/molecules25081999>

393 Wang X, Li Y, Deng Y, et al (2016) Contributions of Basic Chemical Components to  
394 the Mechanical Behavior of Wood Fiber Cell Walls as Evaluated by Nanoindentation.  
395 *BioResources* 11:6026–6039. <https://doi.org/10.15376/biores.11.3.6026-6039>

396 Wang X, Li Y, Wang S, et al (2017) Temperature-dependent mechanical properties of  
397 wood-adhesive bondline evaluated by nanoindentation. *The Journal of Adhesion*

398 93:640–656. <https://doi.org/10.1080/00218464.2015.1130629>

399 Wang X, Song L, Cheng D, et al (2019b) Effects of saturated steam pretreatment on the  
400 drying quality of moso bamboo culms. *Eur J Wood Prod* 77:949–951.  
401 <https://doi.org/10.1007/s00107-019-01421-y>

402 Wang X, Yuan Z, Zhan X, et al (2020b) Multi-scale characterization of the thermal –  
403 mechanically isolated bamboo fiber bundles and its potential application on engineered  
404 composites. *Construction and Building Materials* 262:120866.  
405 <https://doi.org/10.1016/j.conbuildmat.2020.120866>

406 Wang X, Zhao L, Deng Y, et al Effect of the penetration of isocyanates (pMDI) on the  
407 nanomechanics of wood cell wall evaluated by AFM-IR and nanoindentation (NI). 9

408 Wang X, Zhao L, Xu B, et al (2018) Effects of accelerated aging treatment on the  
409 microstructure and mechanics of wood-resin interphase. *Holzforschung* 72:235–241.  
410 <https://doi.org/10.1515/hf-2017-0068>

411 Yang L, Lou Z, Han X, et al (2020) Fabrication of a novel magnetic reconstituted  
412 bamboo with mildew resistance properties. *Materials Today Communications*  
413 23:101086. <https://doi.org/10.1016/j.mtcomm.2020.101086>

414 Yuan T, Liu J, Hu S, et al (2021) Multi-scale characterization of the effect of saturated  
415 steam on the macroscale properties and surface changes of moso bamboo. 11:9

416 Yuan Z, Wu X, Wang X, et al (2020) Effects of One-Step Hot Oil Treatment on the  
417 Physical, Mechanical, and Surface Properties of Bamboo Scrimber. *Molecules* 25:4488.  
418 <https://doi.org/10.3390/molecules25194488>

419 Zhang YM, Yu YL, Yu WJ (2013) Effect of thermal treatment on the physical and  
420 mechanical properties of phyllostachys pubescen bamboo. *Eur J Wood Prod* 71:61–67.  
421 <https://doi.org/10.1007/s00107-012-0643-6>

422 Zhu W, Yao Y, Zhang Y, et al (2020) Preparation of an Amine-Modified Cellulose  
423 Nanocrystal Aerogel by Chemical Vapor Deposition and Its Application in CO<sub>2</sub>  
424 Capture. *Ind Eng Chem Res* 59:16660–16668. <https://doi.org/10.1021/acs.iecr.0c02687>

425